~~Intrinsic non-stationarity of carbon dioxide turbulent fluxes in the urban boundary layer~~

Lei Liu[1], Yu Shi[1], and Fei Hu[1,2]

[1]LAPC, Institute of Atmospheric Physics, Chinese Academy of Sciences, Beijing 100029
[2]University of Chinese Academy of Sciences, Beijing, 100049

Correspondence: Fei Hu (hufei@mail.iap.ac.cn)

Abstract. Stationarity is a critical assumption in the eddy-covariance method that is widely used to calculate turbulent fluxes. Many methods have been proposed to diagnose non-stationarity attributed to external non-turbulent flows. In this paper, we focus on intrinsic non-stationarity (IN) attributed to turbulence randomness. The detrended fluctuation analysis is used to quantify IN of CO_2 turbulent fluxes in the downtown of Beijing. Results show that the IN is ~~widespread~~ common in CO_2 turbulent fluxes and is a small-scale phenomenon related to the inertial sub-range turbulence. The small-scale IN of CO_2 turbulent fluxes can be simulated by the Ornstein-Uhlenbeck (OU) process as a first approximation. Basing on the simulation results, we find that the ~~average~~ time should be greater than 27 s to avoid the effects of IN. Besides, the non-stationarity diagnosis methods that do not take into account IN would possibly make a wrong diagnosis with some parameters.

1   Introduction

~~The global warming has gained much attention in recent years because it could induce global climate changes with increasing possibility of extreme climate and weather events and with potential impacts on biodiversity and eco-systems IPCC (2018). The reduction of anthropogenic greenhouse gas emissions is critical to avoid global warming and potential climate change risks. More than half of the population in the world lives in cities UNDESA (2014) and a high proportion of the total anthropocentric greenhouse gas emissions comes from cities Satterthwaite (2008). Thus, cities play a key role in the action of greenhouse gas removal.~~

~~Carbon dioxide is the most important anthropocentric greenhouse gas. A better understanding of the carbon dioxide transport is helpful to make an optimal reduction plan of carbon dioxide emissions in cities Oke et al. (2017).~~ The vertical transport of carbon dioxide in the urban boundary layer, dominated by turbulence, is quantified by the turbulent flux which is normally obtained by the eddy-covariance method using high frequency wind velocity and carbon dioxide concentration observations Stull (1988):

$$w'c' = (w - \langle w \rangle)(c - \langle c \rangle), \tag{1}$$

where $w'c'$ is the instantaneous turbulent flux of carbon dioxide, w is the vertical wind velocity, c is the carbon dioxide concentration, and $\langle w \rangle$ and $\langle c \rangle$ are the corresponding Reynolds averages. The notation $\langle \cdot \rangle$ denotes the ensemble average, i.e., averaging data collected from many independent experiments with the same conditions. It is difficult to calculate ensemble average in practice. However, if data are nearly stationary and the average time is long enough, the ensemble average can be estimated by the time average Stull (1988); Lenschow et al. (1994). Therefore, stationarity is a critical assumption for the eddy-covariance method and many methods are proposed to diagnose non-stationarity in the time series of instantaneous turbulent fluxes before calculating their averages Foken and Wichura (1996).

The non-stationarity attributed to various non-turbulent flows or external forcings has gained much attention in the literature (Mahrt and Bou-Zeid, 2020, and references therein). The non-turbulent flows or external forcings include the time changes of surface heat fluxes Halios and Barlow (2018); Angevine et al. (2020), the time-dependent horizontal pressure gradients Momen and Bou-Zeid (2017), the sub-meso motions in the stable boundary layer Mahrt (2014); Sun et al. (2015); Cava et al. (2019); Stefanello et al. (2020), and so on. In fact, there is another kind of non-stationarity attributed to randomness. This kind of non-stationarity would not disappear even if the non-turbulent flows or the external forcings are absent or removed and is thus called the diffusion-like intrinsic non-stationarity or intrinsic non-stationarity (IN) Höll et al. (2016). To our knowledge, the IN of carbon dioxide fluxes is less noticed. In this paper, we focus on the IN of carbon dioxide turbulent fluxes in the urban boundary layer. We firstly illustrate the IN by a simple stochastic model in Sec. 2.1. Then, a method, called the detrended fluctuation analysis used to detect and quantify the IN in time series, is briefly introduced in Sec. 2.2. In Secs. 3.1 and 3.2, the IN of carbon dioxide turbulent fluxes in the urban boundary layer are analyzed and simulated. At last, we discuss the possible impacts of the IN on the calculation of carbon dioxide fluxes in Sec. 3.3.

2 Method and Data

2.1 Illustration of intrinsic non-stationarity

The intrinsic non-stationarity (IN) can be simply illustrated by the Brownian motion. A discrete time series of the Brownian motion is generated by cumulatively summing the independent Gaussian samples with zero mean and the same standard deviation σ Lawler (2018):

$$B(t = N\Delta t) = \sum_{i=0}^{N} g_i, \tag{2}$$

where g_i is a Gaussian sample and Δt is the sampling interval. The Brownian motion $B(t)$ is non-stationary because its standard deviation scales as $\sigma\sqrt{t}$.

Two discrete time series of the Brownian motion are shown in Fig. 1a. The two series are generated by the same Brownian motion, i.e., the statistical distributions of g_i are the same for the two series. However, they have different non-stationary trends: the sample A has a decreasing trend from $t \approx 10^4$ while the sample B has a wave-like trend. We call these non-stationary trends the stochastic trends because it is not attributed to any external forcings but only attributed to randomness of the time series.
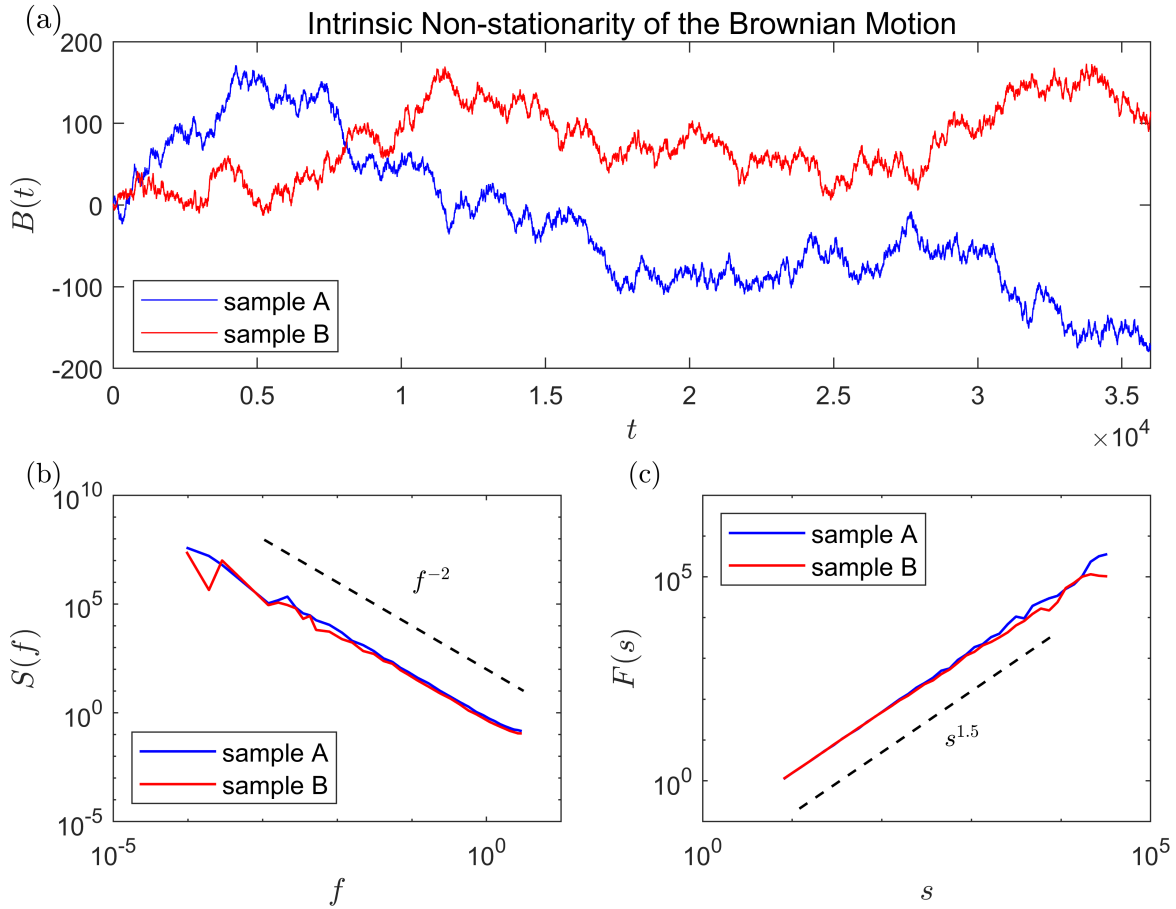
Figure 1. Illustration of intrinsic non-stationarity by the Brownian motion: (a) Two time series of the Brownian motion. The standard deviation of g_i in Eq. (2) is set to 1. The time series length is 36000. (b) The spectra analysis of the two series, where the power spectral density $S(f)$ is plotted as a function of frequency f. (c) The detrended fluctuation analysis of the two series, where the fluctuation functions $F(s)$ is plotted as a function of time scale s. The theoretical predictions are shown by broken line in panels (b) and (c).

As a distinction, the non-stationary trends related to external forcings are called the dynamical trends. Although the stochastic trends are different, the power spectral densities $S(f)$ of two time series are not changed (see Fig. 1b): both of them agree well with the theoretical prediction that $S(f) \sim f^{-2}$ Krapf et al. (2018). Unlike the stochastic trends, different dynamical trends indicate that systems would probably be dominated by different external forcings and the corresponding power spectral densities could also be different.

2.2 Detrended fluctuation analysis

The intrinsic non-stationarity (IN) in a time series can be detected and quantified by the fluctuation analysis Peng et al. (1992). The IN and non-stationarity by external forcings always coexist in a real time series. Thus, an improved method, called the detrended fluctuation analysis (DFA) Kantelhardt et al. (2001), was proposed to resolve this problem.

The DFA of a time series x_k ($k = 1, 2, \cdots, N$) is briefly listed as follows. In the first step, the profile of x_k is calculated by

$$Y_i = \sum_{k=1}^{i} x_k - \bar{x}, \tag{3}$$

where $\bar{x}$ is the time average of x_k over the whole time period. In the second step, the profile Y_i ($i = 1, 2, \cdots, N$) is cut into N_s non-overlapping segments with equal time scale $s = m\Delta t$, where Δt is the sampling interval of x_k and m is a positive integer. In the third step, the profile Y_i in each segment is fitted by a polynomial $p_{i,j}^n$, where j is the segment index and n is the degree of the polynomial. Then, the fitted polynomial in each segment is removed from the profile:

$$Y_{i,j} = Y_i - p_{i,j}^n. \tag{4}$$

In this step, the dynamical trends modeled by the polynomials are removed, but the IN stochastic trends are left Höll et al. (2016). Generally, the choice of degree n would affect the results when dynamical trends exist in the time series. However, we test the Brownian motion without dynamical trends and the carbon dioxide fluxes with dynamical trends already removed by the Reynolds average and find that the results are not significantly affected by the choice of n. Figure 2 shows the impact of the choice of n on DFA. Results show that the choice of n from 1 to 4 does not affect the conclusion of the DFA (Fig. 2a). For the Brownian motion, the fluctuation exponents are almost the same with different degrees n. For the carbon dioxide turbulent fluxes, the variations of the fluctuation functions also do not vary significantly with n (Fig. 2b). Thus, we set $n = 1$ in this study. In the fourth step, the variance of $Y_{i,j}$ in each segment is calculated by

$$F_j^2 = \frac{1}{m} \sum_{i=1}^{m} Y_{(j-1)m+i,j}^2. \tag{5}$$

Then, the variance F_j^2 is averaged over all segments:

$$F(s) = \sqrt{\frac{1}{N_s} \sum_{j=1}^{N_s} F_j^2}, \tag{6}$$

where $F(s)$ is called the fluctuation function.

Generally, the fluctuation function behaves as a power function:

$$F(s) \sim s^{\alpha}, \tag{7}$$

where the fluctuation exponent α can be used to diagnose and quantify IN in the time series of x_k Kantelhardt (2012); Løvsletten (2017). If $\alpha > 1$, the IN exists in the time series. The more the α deviates from 1, the more significant the IN is. If
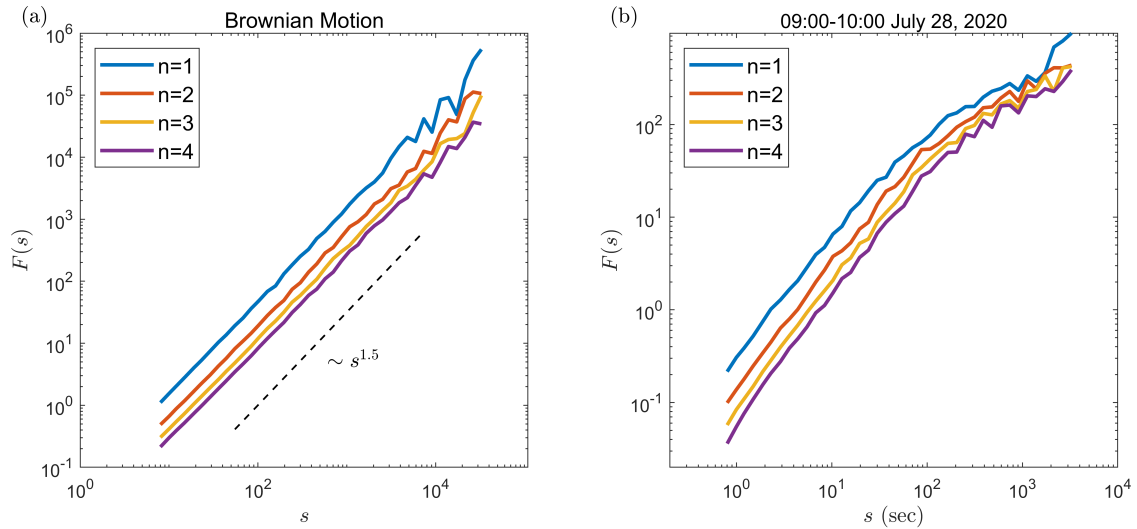
Figure 2. The DFA of (a) the Brownian motion and (b) the 1-hr time series of carbon dioxide turbulent fluxes with the Reynolds average time of 900 s. The results with different degrees n of the polynomial in the DFA are shown by different color lines clarified in the legend. For the Brownian motion, the standard deviation of g_i (see Eq. 2) is set to 1. The broken line indicates the theoretical prediction Höll and Kantz (2015).

$1/2 < \alpha < 1$, the time series is stationary and long-term correlated. If $\alpha = 1/2$, the time series is stationary and independent (or short-term correlated). Figure 1c shows the DFA of the Brownian motion. The fluctuation exponent is close to the theoretical value of 1.5 Höll and Kantz (2015), which is consistent with the fact that the Brownian motion has IN. Besides, the example also shows that the IN will not be removed in the third step of the DFA.

2.3 Data

The data were collected on a 325-m meteorological tower in the downtown of Beijing, China (39.97 °N, 116.37 °E). Within 5 kilometers of the tower, there are buildings with a height of about 10-60 m. About 200 m away to the west of the tower, there are a north-south highway bridge and a ring road. About 150 m away to the north of the tower, there is an east-west busy road. The 10-Hz turbulence data, including wind velocity and carbon dioxide concentration, were collected by an ultrasonic anemometer (Windmaster Pro, Gill, UK) and an open path CO_2/H_2O analyzer (LI-7500, LI-COR, USA) deployed at the 80-m level. Data collected from July 28, 2020 to August 28, 2020 are analyzed in this study. More details about the meteorological tower are referred to the literature Cheng et al. (2018); Liu et al. (2021).

~~The quality control methods, proposed by Vickers and Mahrt (1997) and including spikes, dropouts, data with discontinuities, data violating absolute limits, data with the amplitude resolution problem, data with unphysical high-order moments, are used to find problematic data.~~ The time series seriously contaminated by the problematic data are removed in the analysis. The time series seriously contaminated by high-frequency white noises are also removed. After quality controlling, a total of 520 1-hr

95 time series are left. The instrument reference frame is transformed to the streamline reference frame by the double rotation Kaimal and Finnigan (1994).

3 Results

3.1 Characteristics of intrinsic non-stationarity of carbon dioxide fluxes

The 1-hr time series of carbon dioxide turbulent fluxes is obtained by Eq. (1), where the ensemble average is replaced by the
100 time average. In order to remove dynamical trends, the Reynolds average time is usually set to equal or be smaller than 30 minutes Foken et al. (2004). We analyze the intrinsic non-stationarity for all the 1-hr time series of carbon dioxide turbulent fluxes, and a typical example is shown in Fig. 3.

~~We here choose the Reynolds average time $\tau = 900$ s, 300 s, 6 s to analyze the impact of the Reynolds average time on IN in the 1-hr time series of carbon dioxide turbulent fluxes.~~ The DFA is shown in Fig. 3b. Two scaling regimes are found in
105 the fluctuation functions. At large time scale s, the fluctuation exponent is found to be less than 1; at small time scale s, the fluctuation exponent is found to be greater than 1. Results indicate that the time series of carbon dioxide turbulent fluxes have IN at small time scales but are stationary at large time scales, whatever the Reynolds average time is. As shown in Fig. 3a, the small-scale variations of these time series are evidently non-stationary, although the large-scale dynamical trends have been removed by subtracting the Reynolds average from data. Besides, one can note that the fluctuation functions with $\tau = 900$ s
110 and 300 s are almost the same but are different from that with $\tau = 6$ s. The crossover scale in the case with $\tau = 6$ s (at $s \approx 2$ s) is smaller than that in cases with $\tau = 900$ s and 300 s (at $s \approx 20$ s). The power spectral densities of these time series are shown in Fig. 3c. The spectra with $\tau = 900$ s and 300 s are almost the same but are also different from that with $\tau = 6$ s. The case with $\tau = 6$ s is found to have a much shorter inertial sub-range than cases with $\tau = 900$ s and 300 s. The inertial sub-range is recognized by the Kolmogorov $-5/3$ law Kolmogorov (1941). Results indicate that the IN is a small-scale phenomenon which
115 is intimately related to the inertial sub-range turbulence. The choice of very small Reynolds could partly remove the IN, but the turbulence contribution to fluxes is also partly removed.

3.2 Simulation of intrinsic non-stationarity

The Ornstein-Uhlenbeck (OU) process, that is well-studied and used to model many physical and chemical processes Gardiner (1985), is a simple model of small-scale intrinsic non-stationarity (IN). The discrete time series of the OU process is generated
120 by the iterative equation:

$$y(t + \Delta t) = y(t) - ay(t)\Delta t + b\sqrt{\Delta t}\xi, \tag{8}$$

where a and b are model parameters, Δt is the sampling interval, and ξ is an independent random variable with the normal distribution. For the OU process, the fluctuation function $F(s) \sim s^{0.5}$ at large scales and $F(s) \sim s^{1.5}$ at small scales Höll and Kantz (2015); Czechowski and Telesca (2016); Løvsletten (2017). This indicates that the OU process has IN at small scales but is stationary at large scales, as clearly illustrated by an example in Figs. 4 and 5. Figure 4a shows the 1-hr time series of the
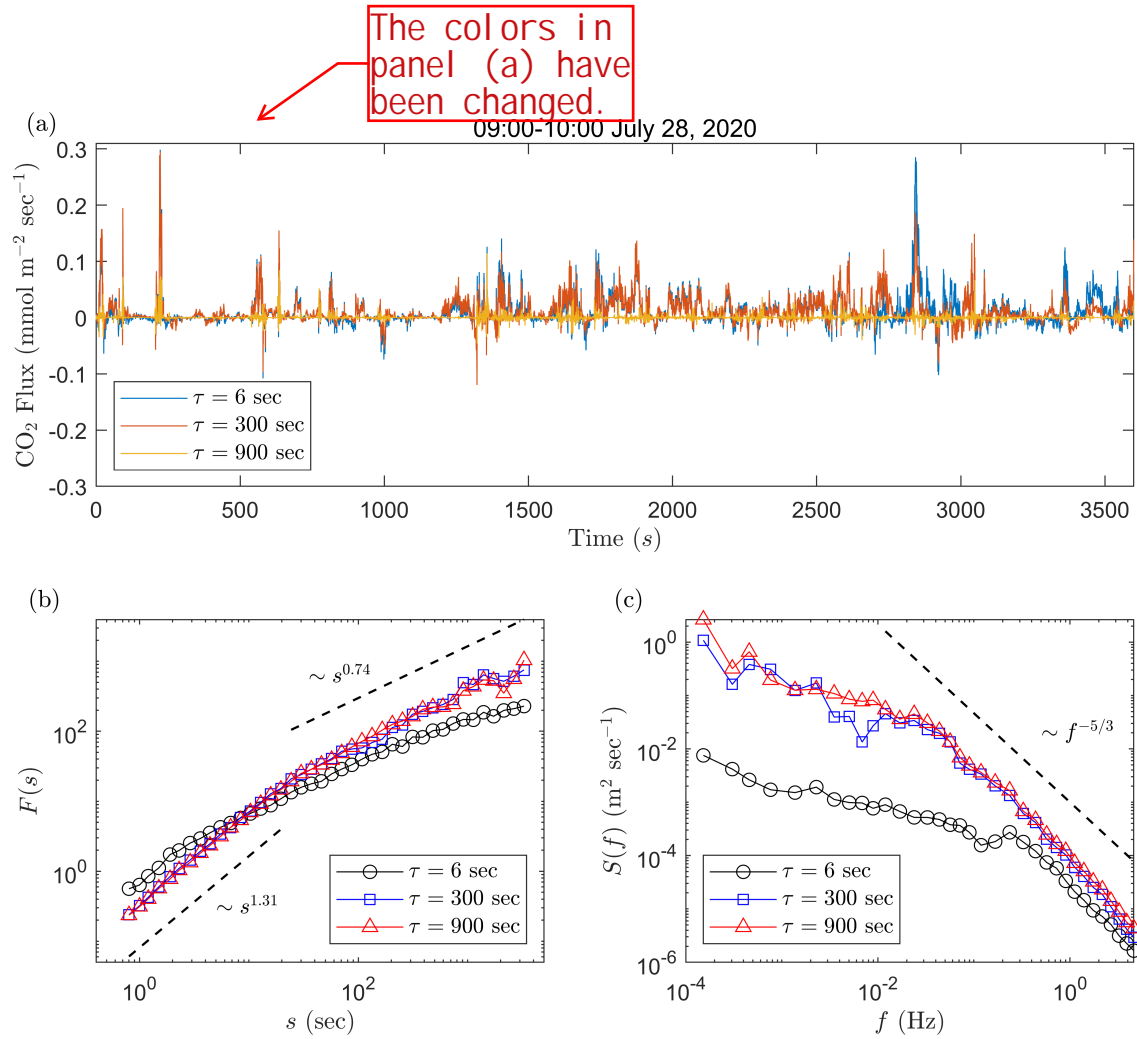
Figure 3. The intrinsic non-stationarity in the 1-hr time series of carbon dioxide turbulent fluxes: (a) The 1-hr time series of instantaneous turbulent fluxes of carbon dioxide with the Reynolds average time τ=900 s, 300 s, and 6 s. (b) The detrended fluctuation analysis of these time series. For comparison, the time series are normalized to zero mean and unit variance. The power functions with the fitted fluctuation exponents are shown by the broken lines. (c) The power spectral densities of these time series. The Kolmogorov $-5/3$ law is shown by the broken line.
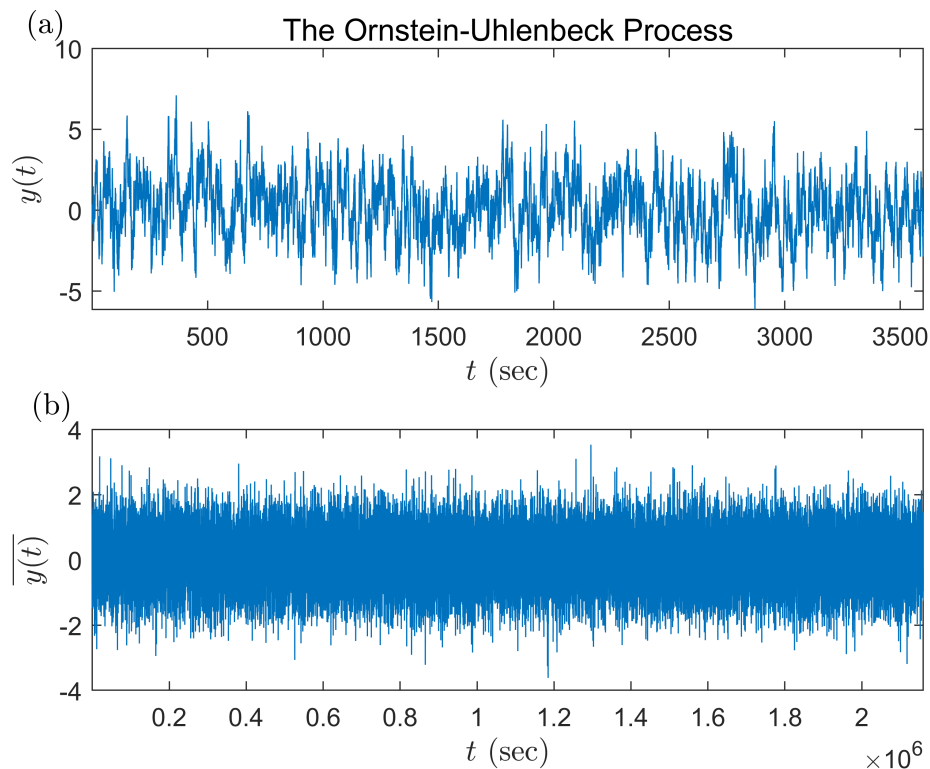
Figure 4. Small-scale non-stationarity and large-scale stationarity in the same OU process. (a) The 1-hr time series of the OU process with $a = 0.15$, $b = 1$, and $\Delta t = 0.1$ s. (b) The average time series of the OU process with the same parameters as in (a). The average time is set to 1 min.

125   OU process generated by Eq. (8). Due to the small-scale IN, the time series seems to be intermittent. However, the large-scale variations of the same OU process, obtained by averaging the time series in Fig. 4a with an average time much greater than the crossover scale, seem to be like a stationary white noise (Fig. 4b). The DFA shows that the fluctuation exponent of the averaged time series is about 0.5, as the fluctuation exponent of the unaveraged time series at large scales (Fig. 5). This indicates that the averaged time series with a large average time, reflecting the large-scale variations of the OU process, is stationary.

130   The DFA of 520 1-hr time series of instantaneous carbon dioxide fluxes is shown in Fig. 6. The Reynolds average time is set to 5 min. Results show that the fluctuation functions of carbon dioxide turbulent fluxes typically have two scaling regimes, as shown in Fig. 3. The fluctuation exponents are generally greater than 1 at small scales and less than 1 at large scales. The OU process can fit the data as a first approximation, although the fluctuation exponent of data seems to be greater at large scales and less at small scales, compared with the OU process. The details of fitting procedure are listed as follows. In the first step,

135   choose the parameters of the OU process a and b from the same set $(0.1, 0.2, \cdots, 1)$, and set $\Delta t = 0.1$ s. The 1-hr time series of the OU process is generated by Eq. (8) with the chosen parameters. In the second step, compute the fluctuation function
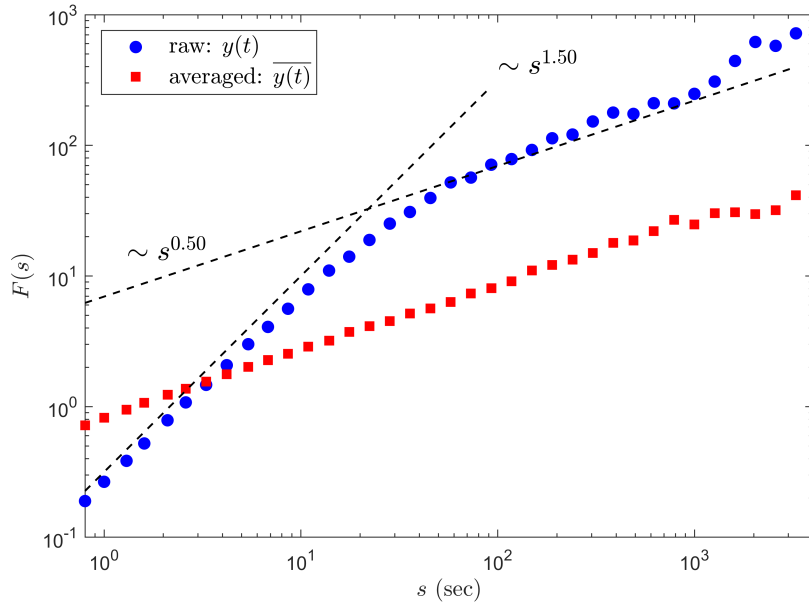
Figure 5. The DFA of the time series shown in Fig. 4. The fluctuation functions of the unaveraged and averaged time series are denoted by blue circles and red rectangles respectively. The theoretical predictions of the OU process are also denoted by broken lines Höll and Kantz (2015); Czechowski and Telesca (2016); Løvsletten (2017).

of the generated 1-hr time series. In the third step, go back to the first step and choose another new value of a or b in the set $(0.1, 0.2, \cdots, 1)$. If all possible combinations of a and b are used, go to the fourth step. In the fourth step, the root mean relative square error for the i-th combination of a and b is computed:

$$RMRS_i = \sqrt{\frac{1}{N_j} \sum_{j=1}^{N_j} \left[\frac{F_i(s_j) - F_{data}(s_j)}{F_i(s_j)} \right]^2}, \tag{9}$$

where N_j is the number of discrete time scale s_j, F_i is the fluctuation function of the OU process with the i-th combination of a and b, and F_{data} is the averaged fluctuation function of carbon dioxide turbulent fluxes (shown by the red line in Fig. 6). In the fifth step, the parameters of a and b corresponding to the minimum of $RMRS_i$ are considered as the optimal fitting parameters. ~~Some kind of extension of the OU process could give a better fitting; however, we only focus on the main characteristics of IN in this paper and the improved fittings would be studied in future work.~~

3.3 Impacts of intrinsic non-stationarity on flux calculation

There are at least two impacts of intrinsic non-stationarity (IN) on the calculation of average carbon dioxide turbulent fluxes.

First, the IN could affect the short-term averaged turbulent flux normally used in the analysis of plant photosynthesis efficiency Van Kesteren et al. (2013). To avoid IN at small scales, the average time averaging instantaneous turbulent fluxes (i.e., the flux-averaging time) should be much greater than the crossover scale in the fluctuation function, because crossover
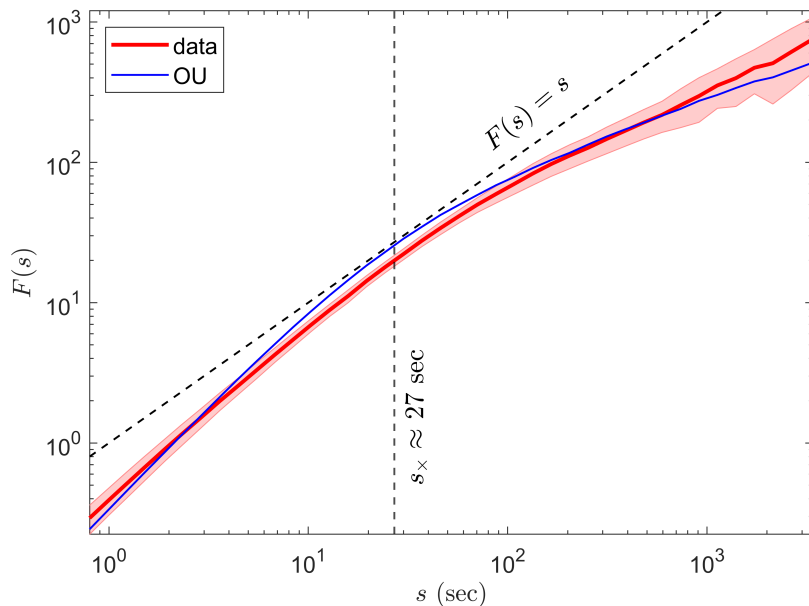
Figure 6. The detrended fluctuation analysis of all 1-hr time series of carbon dioxide fluxes. The Reynolds average time is set to 5 min to calculate fluxes. The sample-averaged fluctuation function is shown by the red line and uncertainties estimated by the standard deviation are shown by the red shading. The fitted fluctuation function of the Ornstein-Uhlenbeck (OU) process is shown by the blue line. The fitted parameters $a = 0.2$, $b = 0.7$, and $\Delta t = 0.1$ s. The vertical broken line indicates the crossover scale estimated by Eq. (10). For comparison, the function of $F(s) = s$ is also shown by the broken line.

scale separates the IN at small scales and stationarity at large scales. Note that the flux-averaging time is not necessarily the same as the Reynolds average time Foken et al. (2004). The former is denoted by T in the following discussion. For the Ornstein-Uhlenbeck (OU) process Czechowski and Telesca (2016), the crossover scale

$$s_\times \approx \frac{5.4}{a}. \tag{10}$$

According to the fitting results in Fig. 6, the crossover scale of carbon dioxide turbulent fluxes is about 27 s. The errors of
155   fluxes averaged with $T \lesssim s_\times \approx 27$ s would be large due to the existing of small-scale IN.

Second, the IN could affect the diagnosis methods of non-stationarity. For example, Vickers and Mahrt (1997) have used a dimensionless index RN to diagnose non-stationarity:

$$RN = \frac{\delta x}{\bar{x}}, \tag{11}$$

where δx is the difference between the beginning and the end of linear regression trend of the diagnosed time series and $\bar{x}$ is the time average of the same time series. If RN is greater than a predefined threshold, the time series is diagnosed as non-
160   stationary and are not recommended to be averaged by time. We here use the RN-method to the OU process. Because the OU process is stationary at large scales, it is meaningful to calculate its average with a large average time. Thus, we hope that the
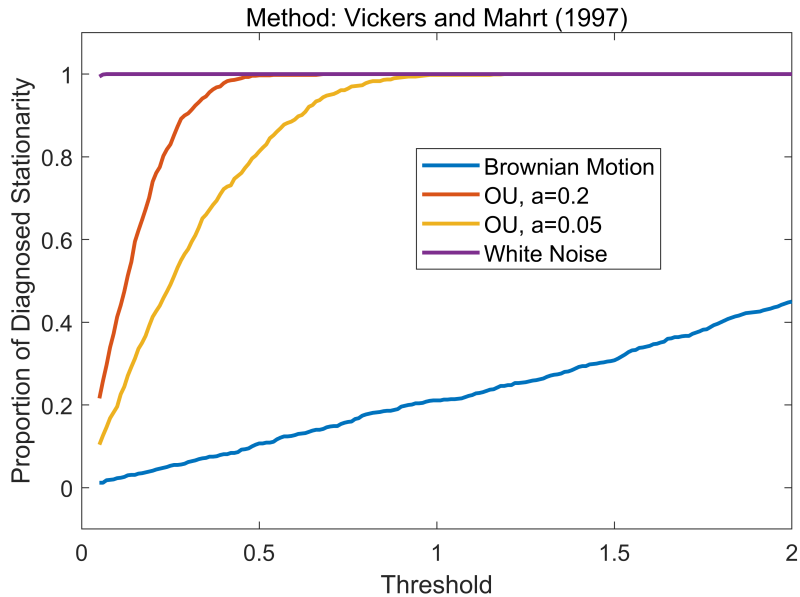
Figure 7. The impact of IN on the non-stationarity diagnosis method proposed by Vickers and Mahrt (1997). The proportion of diagnosed stationarity is plotted as a function of threshold. The functions for the white noise, the OU process with $a = 0.2$ and $b = 0.7$, the OU process with $a = 0.05$ and $b = 0.7$, and the Brownian motion are shown by different color lines, as listed in the legend. The number of generated time series of each model is 1000. To avoid zero denominator in Eq. (11), the averages of all generated time series are set to 1.

OU process can be diagnosed as stationary by the RN-method. The proportion of diagnosed stationarity for the OU process is plotted as a function of threshold in Fig. 7. Results show that once the threshold is less than a critical value the RN-method has a certain probability to make wrong diagnosis. With the decrease of the threshold, the probability of misdiagnosis will increase. The critical threshold increases as the parameter a decreases. In the limit case with $a = 0$, the OU process with small-scale IN becomes the Brownian motion with full-scale IN (see Eq. 8). We thus hope that the proportion of diagnosed stationarity for the Brownian motion is 0; however, the RN-method has the probability of misdiagnosis almost at any threshold. In another limit case of the white noises without non-stationarity, the RN-method performs well and the probability of misdiagnosis is 0 for most thresholds. The results remind us that the parameters of diagnosis methods must be carefully chosen when diagnosing carbon dioxide fluxes with IN.

4   Conclusions

We analyze the time series carbon dioxide fluxes observed by the eddy-covariance system in the downtown of Beijing and find a new kind of non-stationarity less discussed in the literature. As illustrated by the Brownian motion, the new kind of non-stationarity has nothing to do with non-stationarity attributed to non-turbulent flows or external forcings; therefore, it is called the intrinsic non-stationarity (IN). The detrended fluctuation analysis (DFA) is a useful method to measure IN in real time series

where IN always coexists with non-stationarity by external forcings. The DFA shows that the instantaneous turbulent fluxes of carbon dioxide have IN at small time scales. Combined with the spectral analysis, the IN is found to be related to inertial sub-range turbulence. The small-scale IN can be simulated by the Ornstein-Uhlenbeck (OU) process as a first approximation. The potential impacts of IN on the calculation of turbulent fluxes are also discussed. According to the OU process, the crossover scale, that is the characteristic scale under which the IN cannot be ignored, is estimated to be about 27 s. Thus, the IN could contribute systematical errors to short-term averaged fluxes when the average time is not much greater than the crossover time. Besides, we also find that there may be a probability of misdiagnosis when applying some non-stationarity diagnosis method to the time series with IN. Thus, IN should be seriously considered when designing new diagnosis methods.

This work only focuses on the main characteristics of IN of carbon dioxide fluxes in the urban boundary layer. The parameterizations of IN characteristics, such as the crossover scale and fluctuation exponents, with the urban boundary layer parameters should be systematically studied. The extensions of the OU process should be tried to obtain a better fitting with data. Except for the carbon dioxide turbulent flux, is there IN in other turbulent flux? The above problems remain to be resolved in the future study.

Code and data availability. The Matlab code of the DFA is provided by Martin Magris (downloadable at https://www.mathworks.com/matlabcentral/fileexchange/67889-detrended-fluctuation-analysis-dfa). A total of 520 1-hr time series of carbon dioxide turbulent fluxes used in this study are available online at https://doi.org/10.4121/14790084.v1

Author contributions. FH and LL conceived the idea; LL finished all analysis and wrote the manuscript; YS contributed to revise the manuscript and edit the plots. All authors contributed to the interpretation of the results.

Competing interests. The authors declare that they have no conflict of interest.

Acknowledgements. This work was supported by the National Natural Science Foundation of China (Grant 41975018) and the General Financial Grant from the China Postdoctoral Science Foundation (2020M670420).

References

Angevine, W. M., Edwards, J. M., Lothon, M., LeMone, M. A., and Osborne, S. R.: Transition periods in the diurnally-varying atmospheric boundary layer over land, Boundary-Layer Meteorology, 177, 205–223, 2020.

200 Cava, D., Mortarini, L., Giostra, U., Acevedo, O., and Katul, G.: Submeso motions and intermittent turbulence across a nocturnal low-level jet: A self-organized criticality analogy, Boundary-Layer Meteorology, 172, 17–43, 2019.

Cheng, X. L., Liu, X. M., Liu, Y. J., and Hu, F.: Characteristics of CO2 Concentration and Flux in the Beijing Urban Area, Journal of Geophysical Research: Atmospheres, 123, 1785–1801, 2018.

Czechowski, Z. and Telesca, L.: Detrended fluctuation analysis of the Ornstein-Uhlenbeck process: Stationarity versus nonstationarity, Chaos:
205 An Interdisciplinary Journal of Nonlinear Science, 26, 113 109, 2016.

Foken, T. and Wichura, B.: Tools for quality assessment of surface-based flux measurements, Agricultural and Forest Meteorology, 78, 83–105, 1996.

Foken, T., Göockede, M., Mauder, M., Mahrt, L., Amiro, B., and Munger, W.: Post-field data quality control, in: Handbook of micrometeorology, pp. 181–208, Springer, 2004.

210 Gardiner, C. W.: Handbook of stochastic methods for Physics, Chemistry and the Natural Sciences, Springer, 1985.

Halios, C. H. and Barlow, J. F.: Observations of the morning development of the urban boundary layer over London, UK, taken during the ACTUAL project, Boundary-layer Meteorology, 166, 395–422, 2018.

Höll, M. and Kantz, H.: The fluctuation function of the detrended fluctuation analysis—investigation on the AR (1) process, The European Physical Journal B, 88, 1–9, 2015.

215 Höll, M., Kantz, H., and Zhou, Y.: Detrended fluctuation analysis and the difference between external drifts and intrinsic diffusionlike nonstationarity, Physical Review E, 94, 042 201, 2016.

IPCC: Global Warming of 1.5 °C, 2018.

Kaimal, J. C. and Finnigan, J. J.: Atmospheric boundary layer flows: their structure and measurement, Oxford university press, 1994.

Kantelhardt, J. W.: Fractal and Multifractal Time Series, in: Mathematics of Complexity and Dynamical Systems, edited by Meyers, R.,
220 Springer, 2012.

Kantelhardt, J. W., Koscielny-Bunde, E., Rego, H. H., Havlin, S., and Bunde, A.: Detecting long-range correlations with detrended fluctuation analysis, Physica A: Statistical Mechanics and Its Applications, 295, 441–454, 2001.

Kolmogorov, A. N.: The local structure of turbulence in incompressible viscous fluid for very large Reynolds numbers, Dokl. Akad. Nauk SSSR, 30, 301–305, 1941.

225 Krapf, D., Marinari, E., Metzler, R., Oshanin, G., Xu, X., and Squarcini, A.: Power spectral density of a single Brownian trajectory: what one can and cannot learn from it, New Journal of Physics, 20, 023 029, 2018.

Lawler, G. F.: Introduction to stochastic processes, Chapman and Hall/CRC, 2018.

Lenschow, D., Mann, J., and Kristensen, L.: How long is long enough when measuring fluxes and other turbulence statistics?, Journal of Atmospheric and Oceanic Technology, 11, 661–673, 1994.

230 Liu, L., Shi, Y., and Hu, F.: Characteristics and similarity relations of turbulence dispersion parameters under heavy haze conditions, Atmospheric Pollution Research, 12, 330–340, 2021.

Løvsletten, O.: Consistency of detrended fluctuation analysis, Physical Review E, 96, 012 141, 2017.

Mahrt, L.: Stably stratified atmospheric boundary layers, Annual Review of Fluid Mechanics, 46, 23–45, 2014.

Mahrt, L. and Bou-Zeid, E.: Non-stationary boundary layers, Boundary-Layer Meteorology, 177, 189–204, 2020.

235 Momen, M. and Bou-Zeid, E.: Analytical reduced models for the non-stationary diabatic atmospheric boundary layer, Boundary-Layer Meteorology, 164, 383–399, 2017.

~~Oke, T. R., Mills, G., Christen, A., and Voogt, J. A.: Urban climates, Cambridge University Press, 2017.~~

Peng, C.-K., Buldyrev, S. V., Goldberger, A. L., Havlin, S., Sciortino, F., Simons, M., and Stanley, H. E.: Long-range correlations in nucleotide sequences, Nature, 356, 168–170, 1992.

240 ~~Satterthwaite, D.: Cities' contribution to global warming: notes on the allocation of greenhouse gas emissions, Environment and Urbanization, 20, 539–549, 2008.~~

Stefanello, M., Cava, D., Giostra, U., Acevedo, O., Degrazia, G., Anfossi, D., and Mortarini, L.: Influence of submeso motions on scalar oscillations and surface energy balance, Quarterly Journal of the Royal Meteorological Society, 146, 889–903, 2020.

Stull, R. B.: An introduction to boundary layer meteorology, Springer Science & Business Media, 1988.

245 Sun, J., Nappo, C. J., Mahrt, L., Belušić, D., Grisogono, B., Stauffer, D. R., Pulido, M., Staquet, C., Jiang, Q., Pouquet, A., et al.: Review of wave-turbulence interactions in the stable atmospheric boundary layer, Reviews of Geophysics, 53, 956–993, 2015.

~~UNDESA: World Urbanization Prospects, 2014.~~

Van Kesteren, B., Hartogensis, O., Van Dinther, D., Moene, A., De Bruin, H., and Holtslag, A.: Measuring H_2O and CO_2 fluxes at field scales with scintillometry: Part II–Validation and application of 1-min flux estimates, Agricultural and Forest Meteorology, 178, 88–105,

250 2013.

Vickers, D. and Mahrt, L.: Quality control and flux sampling problems for tower and aircraft data, Journal of Atmospheric and Oceanic Technology, 14, 512–526, 1997.

The followings are added references:

Celani, A. and Seminara, A.: Large-scale Structure of Passive Scalar, Phys. Rev. Lett., 94, 214 503, 2005.

Donateo, A., Cava, D., and Contini, D.: A Case Study of the Performance of Different Detrending Methods in Turbulent-Flux Estimation, Boundary-Layer Meteorol, 164, 19— 37, 2017.

Doran, J. C.: Characteristics of Intermittent Turbulent Temperature Fluxes in Stable Conditions, Boundary-Layer Meteorology, 112, 241— 255, 2004.

Horgby, A., Segatto, P., E., B., and et al.: Unexpected large evasion fluxes of carbon dioxide from turbulent streams draining the world's mountains, Nat Commun, 10, 4888, 2019

Li, D. and Bou-Zeid, E.: Coherent Structures and the Dissimilarity of Turbulent Transport of Momentum and Scalars in the Unstable Atmospheric Surface Layer., Boundary-Layer Meteorol, 140, 243— 262, 2011.

Liu, L. and Hu, F.: Finescale Clusterization Intermittency of Turbulence in the Atmospheric Boundary Layer, Journal of the Atmospheric Sciences, 77, 2375— 2392, 2020.

Liu, L., Hu, F., and Huang, S. X.: A Multifractal Random-walk Description of Atmospheric Turbulence: Small-scale Multiscaling, Long-tail distribution, and Intermittency, Bound.-Layer Meteor., 172, 351— 370, 2019.

Sean, P. B., John, M. F., and William, J. M.: The effect of static pressure-wind covariance on vertical carbon dioxide exchange at a windy subalpine forest site, Agricultural and Forest Meteorology, 306, 108 402, 2021